

Convective oxygen transport during development in embryos of the snapping turtle *Chelydra serpentina*

Marina R. Sartori^{1,2}, Zachary F. Kohl², Edwin W. Taylor^{3,1}, Augusto S. Abe¹ and Dane A. Crossley II²

¹Departamento de Zoologia, Instituto de Biociências, Universidade Estadual Paulista, Campus Rio Claro, SP, Brazil; ²Department of Biological Sciences, Developmental Integrative Biology Cluster, University of North Texas, Denton, TX 76203-5017, USA; ³School of Biosciences, University of Birmingham, B15 2TT, UK.

Key-words: cardiovascular; blood oxygen content; cardiac output; hemoglobin affinity; reptiles; microspheres distribution

Corresponding author:

Marina Rincon Sartori, PhD

Current address: Department of Clinical Pathology,
Universidade de Campinas (UNICAMP), SP, Brazil.

marinarsartori@gmail.com

List of abbreviations

A-V diff – arteriovenous oxygen content difference
CAM – chorioallantoic membrane
CO – cardiac output
COI – cardiac output index, product of heart rate and heart mass
CaO₂ – arterial oxygen content
CvO₂ – venous oxygen content
 f_H – heart rate
Hb - hemoglobin
Hct – hematocrit
 nH – Hill coefficient / cooperativity coefficient of hemoglobin oxygen binding
PO₂ – oxygen partial pressure
P_{aO2} - arterial partial pressure of oxygen
P_{aCO2} - arterial partial pressure of carbon dioxide
P₅₀ – partial pressure of oxygen at 50% hemoglobin saturation
VO₂ – oxygen consumption rate
O₂ pulse – oxygen pulse, amount of O₂ consumed heart beat⁻¹
%Q – relative blood flow distribution
SaO₂ – Hemoglobin oxygen saturation

ABSTRACT

This study investigated the maturation of convective oxygen transport in embryos of the snapping turtle (*Chelydra serpentina*). Measurements included: mass, oxygen consumption (VO_2), heart rate (f_H), blood oxygen content and affinity and blood flow distribution at 50%, 70% and 90% of the incubation period. Body mass increased exponentially, paralleled by increased cardiac mass and metabolic rate. Heart rate was constant from 50% to 70% of incubation but was significantly reduced at 90%. Hematocrit (Hct) and hemoglobin concentration (Hb) were constant at the three points of development studied but arteriovenous difference (A-V diff) doubled from 50 to 90% of incubation. Oxygen affinity was lower early in 50% of incubation compared to all other age groups. Blood flow was directed predominantly to the embryo but highest to the CAM at 70% incubation and was directed away from the yolk as it was depleted at 90% incubation. The findings indicate that the plateau or reduction in egg VO_2 characteristic of the late incubation period of turtle embryos may be related to an overall reduction in mass-specific VO_2 that is correlated with decreasing relative heart mass and plateaued CAM blood flow. Importantly, if the blood properties remain unchanged prior to hatching, as they did during the incubation period studied in the current investigation, this could account for the pattern of VO_2 previously reported for embryonic snapping turtles prior to hatching.

INTRODUCTION

For developing animals the cardiovascular system is an essential component of the oxygen cascade that supports metabolic rate. A number of key variables allow an organism to regulate this system to meet tissue oxygen demands during development. These include changing cardiac output and blood oxygen content (Tazawa and Mochizuki, 1977; Burggren et al., 2011). The role of the embryonic chorioallantoic membrane (CAM), the primary gas exchange surface (Piiper et al., 1980; Corona and Warburton, 2000) has been studied. However, the ontogeny of key parameters such as stroke volume of the heart, blood oxygen content and selective organ perfusion of most egg laying vertebrates is poorly understood. Quantification of these and other components of convective oxygen transport are necessary to understand how embryos of egg laying species, such as reptiles, adjust oxygen delivery as they progress through development.

Egg oxygen consumption increases with development as the mass of embryonic tissues increase due to growth and differentiation (Thompson, 1989; Booth 1998 a,b; Booth et al., 2000; Crossley et al, 2017a) and the convective oxygen transport system must be sufficient to supply this demand. While components of oxygen delivery have not been extensively investigated in developing animals, metabolic rate has been studied in numerous species representing all reptilian lineages (Lynn and Von Brand, 1945; Dmi'el, 1970; Ackerman, 1981; Thompson, 1989; Booth and Thompson, 1991; Whitehead and Seymour, 1990; Thompson, 1993; Aulie and Kanui, 1995; Birchard and Reiber, 1995; Thompson and Stewart, 1997; Booth, 1998 a, b; Vleck and Hoyt, 1991; Thompson and Russell, 1998; 1999; Booth et al., 2000; Sartori et al, 2017; Crossley et al, 2017a). The patterns of whole egg metabolism in many species are characterized as peaking at some point prior to hatching followed by either a plateau or a decrease (Gettinger et al., 1984; Thompson, 1989; Miller and Packard, 1992; Booth 1998 a,b; Booth et al., 2000; Crossley et al, 2017a). The constant or dropping rate of oxygen consumption during the final period of incubation has been speculated to represent a time allowing for catch up growth and simultaneous hatching in many reptilian species (Spencer et al., 2001). However, this pattern may merely represent a transition in the functional properties of convective transport.

In embryonic reptiles direct measurements of stroke volume and blood oxygen content have never been conducted, however, heart rate and heart mass have been used to estimate cardiac output (Birchard and Reiber, 1996; Crossley and Altimiras, 2005; Nechaeva et al., 2007; Crossley et al., 2017a). Heart mass has been used as a proxy for stroke volume but this approximation has never been validated. Further, when attempting to characterize potential oxygen delivery to tissues using estimates of cardiac output, it is assumed that oxygen content and hemoglobin affinity are constant during development, which may not be the case. In common snapping turtles (*Chelydra serpentina*) embryonic heart rate drops approximately 20% between 70% and 90% of incubation, a change that could result in an overall reduction in cardiac output (Eme et al., 2012; Alvine et al., 2013). Using heart mass as a proxy for stroke volume, a previous study of embryonic snapping turtles reported that cardiac output does not increase in proportion to embryonic mass which would constrain metabolic function (Birchard and Reiber, 1996). This developmental window corresponds to a relative reduction or plateau in metabolic rate in snapping turtles which may be attributed to a reduced convective transport ability (Crossley and Burgreen, 2009). However, changes in blood properties could offset the apparent limit imposed by the cardiovascular system. These could comprise increased hematocrit and hemoglobin content, while changes in oxygen affinity of the hemoglobin could also impact oxygen delivery (Tazawa and Mochizuki, 1977). This study is the first to investigate multiple aspects of convective oxygen transport during the embryonic development of an ectothermic vertebrate. To understand how convective oxygen transport in embryonic snapping turtles changes, we measured oxygen consumption (VO_2), heart rate (f_H) and calculated oxygen pulse (O_2 pulse). We also analyzed blood collected from CAM arteries and veins to quantify blood oxygen content (CaO_2 and CvO_2), hematocrit (Hct), hemoglobin concentration (Hb), and hemoglobin oxygen affinity (P_{50}). Finally we determined relative blood flow ($\%Q_{\text{sys}}$) and estimated cardiac output (CO) of the CAM. We hypothesized that as development progressed embryonic snapping turtles would fuel an increase in metabolic rate, by coordinated changes in convective transport, control of blood flow distribution and increasing levels of oxygen carrying capacity of the blood supplying the developing tissues.

MATERIAL AND METHODS

Eggs from common snapping turtles (*Chelydra serpentina*) were collected in Minnesota and transported to the Biology Department at the University of North Texas. Upon arrival, eggs were labelled, weighed and placed in plastic boxes (approximately 3 l of volume), containing vermiculite mixed with water in a mass ratio of 1:1. Boxes were enclosed in plastic Ziploc® bags ventilated with humidified atmospheric air at $4 \text{ l} \cdot \text{min}^{-1}$ to maintain the oxygen and water saturation at adequate levels. The bags were held in a walk-in environmental chamber set to 30°C . Water content of the vermiculite was maintained by weighing boxes three times a week and water was added as needed. A total of 104 eggs were used in this study. Eggs were taken from incubation at 50%, 70% and 90% (total incubation 53 days) weighed and assigned for measurements of \dot{f}_H , VO_2 , collection of blood or injection of microspheres.

Embryonic heart rate (\dot{f}_H) and oxygen consumption (VO_2) studies

Six embryos from each incubation time were used to determine heart rate. Two silver wire electrodes (26 gauge) were inserted just under the surface of the shell of each egg, and then returned to incubation conditions overnight. The electrode leads were connected to an impedance converter (UFI 2991, Morro Bay, CA) with the output signal connected to a data acquisition system (Powerlab model 8/35). Data was collected at 100Hz using LabChart Pro (V 7.2, AD Instruments, Colorado Springs, CO, USA). Heart rates were recorded for up to an hour in an environmental chamber at $30 \pm 0.5^\circ\text{C}$. The average of three 3-min periods over the final 15 minutes of the recording were used to establish heart rate of each embryo.

The same embryos were then used to determine embryonic oxygen consumption, using a modified version of the closed system respirometry as previously outlined (Crossley et al., 2017b). Briefly, individual eggs were enclosed in hermetically sealed glass chambers (67 ml) with two ports, each connected to a three-way stopcock valve. The valves were closed for a period of 240 min at 50% and 60 min at 70 and 90% of incubation. A 60 ml syringe was connected to one stopcock valve, which was opened for withdrawal of the chamber gas sample (20 ml). Air samples were drawn via a 3-way stopcock

into a 2 m long length of PE-200 tubing open to the room air (a 'reservoir/sipper' system; See Fig. 1 in Warburton et al., 1995 for a schematic of the system). The 3-way stopcock was then opened to the analyzers, and gas samples passed through a 10 cm Drying tube (MLA0343 ADInstruments, CO, USA) in a modified desiccation chamber similar to a desiccant cartridge (MLA6024 ADInstruments, CO, USA). This was connected to gas analyzers in series for measurement of O₂ (S-3A1, Thermox, Ametek, Berwyn, PA, USA) and of CO₂ (CD-3A, Thermox, Ametek, Berwyn, PA, USA). The gas sample was drawn through the analyzers at a rate of 15 ml · min⁻¹. The output from each analyzer was connected to a data acquisition system (Powerlab model 8/35 ADInstruments, CO, USA) and gases concentration data were recorded at 20 Hz using LabChart Pro acquisition software (V 7.2, AD Instruments, Colorado Springs, CO, USA). This procedure was repeated three times, with 10 minutes allowed between samples during which the chambers were opened to restore ambient gas concentrations. Mean VO₂ was calculated based on chamber volume and time. Mass-specific VO₂ (ml O₂ kg⁻¹ min⁻¹) was calculated based on embryo mass that was measured at the completion of all studies (see below). For each egg oxygen pulse (O₂ pulse) was calculated as the amount of whole egg VO₂ per f_H and mass-specific O₂ pulse as mass-specific VO₂ per f_H .

Blood analysis studies

A different group of embryos were used for blood analysis studies. Eggs were removed from incubation and candled to locate either a tertiary artery carrying mixed oxygenated and deoxygenated blood or a vein in the chorioallantoic membrane (CAM) carrying oxygenated blood. Eggs were placed in holders (4 cm diameter) and moved to a temperature-controlled surgical chamber at 30 ± 0.5°C. A portion of the eggshell was removed (~1 cm²) and the targeted chorioallantoic artery or vein was occlusively cannulated under a dissection microscope (Leica MZ6, Leica Microsystems, Waukegan, IL, USA) using a heat-pulled polyethylene tube (PE-50) filled with 0.9% NaCl saline with 50 IU ml⁻¹ heparin, as previously described (Crossley and Altimiras, 2000). A blood sample (approximately 50-80 µl) was immediately taken with a 100 µl Hamilton syringe for analysis.

A fraction of the whole blood was transferred to 50 μ l capillary tube and centrifuged (13,000 rpm) for hematocrit determination (N=13 for 50% and 70%; N=12 for 90%). The remaining fraction, ranging from 11 to 20 μ l, was added to 4 mL of Drabkin's solution and analyzed spectrophotometrically (Shimadzu UV-1800, Cole Parmer, IL, USA) for determination of hemoglobin concentration (N=10 for 50%; N=12 for 70% and N=11 for 90%). Fractions of the blood collected from CAM arteries of 70% and 90% embryos (N=5) were transferred to 60 μ l capillaries, and analyzed in a previously calibrated automatic blood gas analysis system (StatProfile pHox Plus L, Nova Biomedical, Waltham, MA, USA) to measure blood gases (P_{aO_2} and P_{aCO_2}).

For measurement of oxygen content (Tucker, 1967) a fraction of 8-20 μ l of either an arterial or venous blood sample was immediately inserted into a water-jacketed chamber (1.52 ml volume) containing an oxygen electrode (Radiometer, Copenhagen, Denmark) filled with degassed ferrocyanite solution, maintained at 30°C (\pm 0.5°C) via a circulating water bath (VWR International, LLC, West Chester, PA, USA). The oxygen electrode was connected to a PHM 73 gas analyzer (Radiometer, Copenhagen, Denmark) and calibrated with degassed ferrocyanite solution (Tucker, 1967). Three oxygen partial pressure (PO_2) values were recorded, immediately before the injection of the sample in the chamber, and after one and two minutes. The difference between the initial PO_2 value and the mean after injection was used for the calculation of oxygen content (ml O_2 100 ml⁻¹ blood) according to the equation proposed by Tucker (1967). Blood oxygen content values from vessels afferent to and efferent from the CAM were expressed as arteriovenous difference (AV diff) and used to calculate total blood flow (CO) through the CAM (see below).

From a different group of embryos (7 at 50% and 70%; 8 at 90%) a 50 μ l blood sample was diluted with 5 ml of Hemox solution, a manufacturer-provided buffer, and drawn into a cuvette for analysis by an automatic blood oxygen dissociation analyzer (Hemox Analyzer, model B, TCS, New Hope, PA, USA) to determine oxygen binding curves. The system was maintained at 30°C with a circulating water bath (VWR International, LLC, West Chester, PA, USA). After air calibration, the sample was equilibrated with a gas mixture of O_2 with either 2% or 6% CO_2 (G400, Qubit, Kingston, ON, Canada), to simulate respectively, arterial and venous CO_2 conditions. After the air calibration of the

PO₂ value, the sample was deoxygenated with nitrogen, until PO₂ decreased below 0.3 kPa. The output signal was connected to a data acquisition system (Powerlab model 8/35 ADInstruments, CO, USA) at 20 Hz using LabChart Pro acquisition software (V 7.2, AD Instruments, Colorado Springs, CO, USA). Calculation of the Bohr shift was based on $\Delta \log P_{50} / \Delta \log \text{pH}$ under the different conditions of CO₂. We considered that pH would not vary considerably under different Hb-O₂ saturations and used pH values measured with blood collected from 90% embryos diluted in the Hemox buffer which were 7.17 under 2% CO₂ and 6.94 under 6% CO₂.

After all measurements and blood collection, embryos were euthanized with an overdose of isoflurane for measurements of mass of the embryo, heart, liver and yolk to the nearest 0.01 g. Embryonic stage was confirmed by comparison to the staging table of Yntema (1968) for *Chelydra serpentina* embryos. At 50% of the incubation period embryos corresponded to stages 19-20, at 70% to stages 23-24 and at 90% to stage 25. Relative cardiac index (relative COI) was calculated as the product of heart rate and heart mass corrected for embryonic body mass.

Regional blood flow measured by injection of microspheres

A separate group of embryos at each incubation time (5 at 50%; 18 at 70% and 15 at 90%) were injected with colored polystyrene microspheres (Dye Track, Triton Technologies, San Diego, CA, USA) to measure regional blood flow. The microspheres were 15 μm in diameter, larger than the reported size of the snapping turtle red blood cells (Frair, 1977). Instrumentation was similar to that previously reported by our group. Briefly, a tertiary vein of the CAM was catheterized for injection of microspheres as described earlier. Microspheres were suspended in 0.9% saline containing 0.05% Tween 80 (to prevent agglomeration of the microspheres) at a final concentration of 1,500-spheres μL^{-1} . Due to embryonic volume load limitation a total of 52,500 yellow microspheres were injected at 50% incubation and a total of 75,000 at 70% and 90%. The injections were performed with a 100 μL glass Hamilton syringe into the catheterized vein, after a period of stabilization from the microsurgery (approx. 1 hour). At the end of the protocol a blood sample was withdrawn and

stored in a 15 ml Falcon tube in order to detect if any microspheres remained in the circulation. Embryos were euthanized with an intravenous dose of pentobarbital ($50 \mu\text{g kg}^{-1}$). Whole embryo, CAM, and yolk membrane were immediately dissected, weighed and stored in either 15 or 50 ml Falcon tubes. The protocol for recovery of microspheres is described in detail in the guidelines provided by Triton Technologies Inc. and summarized by Stecyk and colleagues (2004). We primarily used the sedimentation method based on a series of centrifugations. Briefly, the sedimentation recovery procedure consists of the following steps: alkaline digestion, a series of washes (Triton X-100, acidified ethanol and ethanol) and elution of the dye. We started tissue digestion with 1 M KOH (Sigma Aldrich, St. Louis, MO) and added 10,000 Blue microspheres to each tube to assess the effectiveness of the recovery process.

Tissues were sonicated to accelerate digestion, using an ultrasonic homogenizer (Fisher Scientific, MA, USA), at 70% of full power for 30s. The digestion step was repeated until a tissue pellet was no longer visible. Samples containing calcified tissue were subjected to additional treatment with a bone digesting reagent (0.12% EDTA, 5.38% HCl, 94% H_2O). For tissues that did not digest after several repetitions of sonication, vortexing, and alkaline digestion (particularly yolk and whole embryo samples) a vacuum filtration method using a 25 mm diameter filter with a $10 \mu\text{m}$ pore size was applied (Triton Technology Part #31079).

After digestion the samples were subjected to a series of washes, and the colored dye was eluted from the microspheres with acidified Cellosolve acetate (Sigma Aldrich). Subsamples of each eluted sample ($175 \mu\text{l}$) were then transferred to a crystal 96-wells plate for dye analysis using a spectrophotometer (Synergy H1, Biotek, VT, USA) at absorbance wavelengths of 650 nm for blue spheres and 440 nm for yellow. To calculate total microspheres and recovery rates for each sample we entered the absorbance values at each wavelength from each tube into a calculation Excel file, provided by the manufacturer. We calculated fractions of blood flow (%Qsys) directed to the vascular bed of the embryo, CAM and yolk considering the total microspheres recovered from the tissues of individual eggs and correcting for the microsphere recovery rate accessed by the blue control spheres.

Estimation of hemoglobin saturation and CAM blood flow

By applying the following oxygen content equation: $Ca_{O_2} = [Hb] \text{ (g·dl}^{-1}\text{)} \times 1.34 \text{ ml O}_2 \text{ g}^{-1}\text{·Hb} \times S_{aO_2} + P_{aO_2} \times (0.003 \text{ ml O}_2\text{·mmHg}^{-1}\text{·dl}^{-1}\text{)}$ to our measured arterial oxygen content (Ca_{O_2}), hemoglobin concentration ($[Hb]$) and oxygen partial pressure (P_{aO_2}) at 70% and 90% we estimated hemoglobin oxygen saturation (S_{aO_2})

By combining our measured CAM A-V difference with the measured values for whole egg VO_2 or mass-specific VO_2 we estimated CAM blood flow (Q_{CAM}) using the Fick equation ($VO_2 = CO \times A\text{-}V \text{ diff}$). Then, Q_{CAM} was determined as the mean VO_2 calculated from one group of embryos divided by the A-V diff calculated with a different group of embryos.

Statistical analysis

Data from oxygen equilibrium curves were plotted as Hill allosteric curves using Graph Pad Prism® software. To measure Hb- O_2 affinity, data were fitted to linear regressions ($r^2 \geq 0.95$) in which PO_2 at 50% Hb saturation (P_{50}) and the corresponding cooperativity coefficient (nH) corresponded to the zero intercept and slope, respectively, of Hill plots $[\log[Y/(1-Y)]]$ versus $\log PO_2$ (where Y is the fractional saturation) fitted to seven saturation steps between 20 and 80%.

All data were tested for differences between the incubation periods using parametric one-way ANOVA but whenever data failed normality or homoscedasticity we used the non-parametric ANOVA on ranks. *Post hoc* tests of Student Newman Keuls or Dunn's were used for detection of differences across groups. For oxygen content a T-test was used to account for differences between arterial and venous blood. The level of significance was established as $P < 0.05$ and data is presented as mean \pm standard error of the mean (s.e.m.). All statistical analyses were conducted with Sigma Plot V 11 software.

RESULTS

Egg masses did not differ between the incubation periods sampled (mean egg mass = 12.9 ± 0.2 g; Table 1), embryonic yolk-free body mass increased 4.4-fold from 1.62 ± 0.08 g at 50% to 7.16 ± 0.16 g at 90% (One-way ANOVA + SNK; $P < 0.001$; Table 1). Liver also increased 4.5-fold from 0.047 ± 0.002 g to 0.213 ± 0.008 g whereas heart mass increased 3-fold from 0.007 ± 0.0002 g to 0.022 ± 0.001 g during the same period (One-way ANOVA + SNK; $P < 0.001$; Table 1). Relative heart mass decreased from $0.46 \pm 0.02\%$ to $0.31 \pm 0.02\%$ (One-way ANOVA + SNK; $P < 0.001$; Table 1).

Heart rate (f_H) decreased from 56 ± 2 beats·min⁻¹ at 50% to 43 ± 3 beats·min⁻¹ at 90% (one-way ANOVA + SNK; $P < 0.001$; Fig. 1A) whereas oxygen consumption (VO_2) of whole eggs increased continuously from $8.5 \times 10^{-3} \pm 5 \times 10^{-4}$ ml O₂ egg⁻¹ min⁻¹ at 50% to $19.9 \times 10^{-3} \pm 7 \times 10^{-4}$ ml O₂ egg⁻¹ min⁻¹ at 90% (One-way ANOVA + SNK; $P < 0.001$; Fig. 1B). Mass-specific metabolic rates decreased progressively from 6.0 ± 0.4 ml O₂ kg⁻¹·min⁻¹ at 50% to 2.8 ± 0.1 ml O₂ kg⁻¹·min⁻¹ (One-way ANOVA + SNK; $P < 0.001$; Fig 1C) as embryonic mass increased. Oxygen pulse, the ratio of oxygen consumed per heart beat, increased from $1.5 \times 10^{-4} \pm 1 \times 10^{-5}$ ml O₂ beat⁻¹ at 50% to $5.0 \times 10^{-4} \pm 4 \times 10^{-5}$ ml O₂ beat⁻¹ at 90% (One-way ANOVA + SNK; $P < 0.001$). When calculated with mass-specific VO_2 , mass-specific O₂ pulse decreased from 0.11 ml O₂ beat⁻¹ kg⁻¹ to 0.07 ml O₂ beat⁻¹ kg⁻¹ (One-way ANOVA + SNK; $P < 0.001$; Fig. 1D).

Blood Values

Hematocrit and hemoglobin concentration did not change between incubation periods and were 22.4 ± 1.3 ml O₂ 100 ml blood⁻¹ and 9.5 ± 0.4 ml O₂ 100 ml blood⁻¹, respectively (Table 2). Partial pressure of blood gases, P_{aO_2} and P_{aCO_2} , from CAM arteries containing mixed oxygenated and deoxygenated blood also did not differ during the periods measured (70 and 90%; Table 2).

Blood O₂ content from the CAM artery, CaO_2 , did not differ between the incubation periods studied (mean of 0.9 ± 0.1 ml O₂ 100 ml blood⁻¹; ANOVA on Ranks; $P = 0.824$) but CAM venous blood O₂ content, CvO_2 , increased from 2.7 ± 0.4 ml O₂ 100 ml blood⁻¹ at 50% to 5.0 ± 0.5 ml O₂ 100 ml blood⁻¹ at 90% of incubation (one-way ANOVA + SNK; $P < 0.05$), resulting in 2-fold increase in the A-V difference (see Fig. 2).

Oxygen equilibrium curves did not differ between 2% and 6% CO₂ conditions in all incubation periods indicating lack of a marked Bohr shift ($F=0.47$; $P=0.7$; Table 2; Fig. 3). At 50% incubation we found two patterns of dissociation curves, which reflected different embryonic stages, although they did not differ statistically in embryonic mass (Table 2). Therefore the period was divided into two subgroups: 'early', which was equivalent to stage 19 of development (50% - E) and 'late', which was equivalent to stage 20 of development (50% - L). Late 50% presented a dissociation curve pattern similar to 70 and 90% and also had similar P_{50} 's. Early 50% had a right shifted curve and a higher P_{50} (lower oxygen affinity) when compared to the late 50%, 70% and 90% incubation (one-way ANOVA + SNK; $P<0.0001$; Table 2; Fig. 3). Hill coefficients (n_H) for 2% and 6% CO₂ curves were all positive (>1) and did not differ between the incubation periods indicating no significant change in the level of hemoglobin cooperativity (one-way ANOVA + SNK; $P=0.41$; Table 2).

Regional blood flow

The distribution of microspheres revealed that relative blood flow directed to the embryonic tissues (% Q_{BODY}), to the chorioallantoic membrane (% Q_{CAM}) and to the yolk sac (% Q_{YOLK}) differed with incubation times (one-way ANOVA + SNK; $P<0.0001$; Fig.4). The blue control spheres added to determine microsphere loss during tissue processing revealed a high efficiency of the recovery process, with rates of $89.76 \pm 0.02\%$ at 50% incubation, 101.79 ± 0.02 at 70% and 103.30 ± 0.02 at 90%.

Throughout the last half of incubation the percentage of blood flow directed to embryonic tissues (% Q_{BODY}) was always greater than the flow to the CAM or to the yolk (Fig 4A-C). The % Q_{BODY} was maximal at 50% (84%) and minimal at 70% of incubation (66%) (Fig 4A-C). The percentage of blood flow directed to the CAM was initially low (9%) at 50% of incubation then rose to 31% and fell to 25% between 70 and 90% of incubation (Fig 4A-C). The relative blood flow directed to the yolk sac was 7% at 50% incubation and progressively decreased upon its depletion (Fig 4A-C), with the small volume of yolk remaining being incorporated into the abdominal cavity before hatching.

Estimation of CAM blood flow (Q_{CAM}) and Hb saturation (SaO_2)

By applying the following equation $CaO_2 = [Hb] (g\ dl^{-1}) \times 1.34\ ml\ O_2\ g\ Hb^{-1} \times S_{aO_2} + P_{aO_2} \times (0.003\ ml\ O_2\ mmHg^{-1}\ dl^{-1})$ to our measured parameters at 70% and 90% we were able to estimate Hb oxygen saturation (S_{aO_2}), which increased from 34% to 49% (Table 3).

When we insert our VO_2 and A-V diff data in the Fick equation ($CO = VO_2/A-V\ diff$) we found that blood flow through the CAM (Q_{CAM}) increases from $0.46\ ml\ min^{-1}$ at 50% to $0.71\ ml\ min^{-1}$ at 70% incubation, but then decreases to $0.50\ ml\ min^{-1}$ at 90% (Fig. 4, Table 2). Instead, when using mass-specific VO_2 , Q_{CAM} decreased from $0.33\ ml\ min^{-1}\ g^{-1}$ at 50% to $0.07\ ml\ min^{-1}\ g^{-1}$ at 90% incubation (Fig. 4; Table 2). In agreement with this last finding, the relative COI also indicated a 50% decrease in total cardiac output from 50 to 90% incubation (Table 2).

DISCUSSION

The development of the components of the convective oxygen transport system, in relation to changes in metabolic rate were largely unknown in reptilian embryos. In this study we found that blood properties were relatively constant throughout snapping turtle incubation, while indexes of cardiac output, relative heart mass, mass-specific metabolic rate and oxygen pulse, decrease over the course of incubation. If this pattern persists during the pre-hatching period (>90% of incubation) it could account for previously reported patterns of whole egg VO_2 in snapping turtle embryos.

Heart rate of snapping turtle embryos decreased significantly at the end of incubation, a common pattern of the Testudine group (Alvine et al., 2013; Birchard and Reiber, 1996; Crossley, 1999; Birchard, 2000; McGlashan et al., 2015; Taylor et al., 2014) and in contrast to the relatively constant f_H during incubation of Squamata (Birchard and Reiber, 1996; Nechaeva et al., 2007; Du et al., 2009; Sartori et al., 2017). In snapping turtles f_H reduction has been related to the onset of parasympathetic tone, which is present at 70% incubation (Alvine et al., 2013), in comparison to the late onset of vagal tone found in green iguana (Sartori et al., 2015) and the lack of vagal tone during incubation in the American alligator (Eme et al., 2011). Heart rate is a critical variable in the adjustment of cardiac output during periods of increased metabolic demand (Joyce et al., 2018) and its decrease, coupled to the

appearance of parasympathetic control, may reflect an overall reduction in tissue demands. Mass specific metabolic rate did fall from 50% and 90% of incubation supporting this speculation (Fig 1D).

Snapping turtle embryos markedly increase in body mass (4.4-fold) during the second half of incubation concurrent to the depletion of the yolk (Table 1). To support this growth egg VO_2 doubled during the last half of the incubation period but f_H decreased by 23%, which results in a 3-fold increase in O_2 pulse. Our previous study in a Squamate reptile, showed that VO_2 varied independently of f_H (Sartori et al., 2017), indicating that other physiological mechanisms were involved in matching O_2 supply to tissue demand during embryonic incubation. In the present study heart mass tripled from 50% to 90% incubation (Fig. 2) However despite the heart growth, the size of the heart relative to the size of the embryo (Table 1) and mass-specific oxygen pulse decreased (Fig. 1). In snapping turtles the size of the heart relative to the size of the embryo was 0.46% at 50% incubation and decreased to 0.31% at 90% (Table 1). This is also the case for the turtles *Emys orbicularis* (from approximately 0.56% at 50% incubation to 0.31% when close to hatching; Nechaeva et al., 2007) and *Lepidochelys olivacea* (from 0.46% at 70% incubation to 0.39% at 90%; Crossley et al., 2017a), and for the lizard *Iguana iguana* (from 0.35% at 30% incubation to 0.26% at 90% incubation; Sartori et al., 2017). This difference in heart growth, when compared to the body mass increase, could be offset to some extent by the reduction in tissue oxygen requirement of the embryo, reflected by the decrease in specific-mass VO_2 (Sartori et al., 2017) and therefore the decrease in mass-specific O_2 pulse (Fig. 1D).

Unlike prior studies we found progressive increases in the VO_2 of snapping turtle eggs during the latter stages of development (Fig. 1B). Previous reports of egg VO_2 for this species demonstrated that VO_2 reached a maximum value before rapid declining immediately prior to hatching (Gettinger et al, 1984; Miller and Packard, 1992; Birchard and Reiber, 1995). While our finding differed, we did not measure VO_2 during the final 10% of incubation which likely contributed to the apparent contradiction with prior work.

Venous blood leaving the CAM, the site of gas exchange, carried more O_2 in embryos at 90% of incubation, which would support the increase in total egg VO_2 (Fig. 2). Factors that would enable the increase in oxygen carrying content of the venous blood could be: I) an increase in the number of red blood cells or in hemoglobin concentration; II) an increased saturation of the hemoglobin, related to the modulation of the hemoglobin oxygen affinity; III) changes in the level of allantoic shunting reducing the levels of deoxygenated blood mixed to the oxygenated blood, IV) increase CAM vascularization and V) decrease in diffusion resistance barrier. We were unable to monitor levels of shunting but found that hematocrit and hemoglobin content remained unchanged throughout the last half of development. Further, with the exception of early 50% of incubation embryos, P_{50} was constant during the last half of the incubation (Table 2; Fig 3). Calculated hemoglobin saturation at 90% was 15% higher than at 70% which likely contributed to the increase in blood oxygen content of blood returning from the CAM (Table 2). While physical measures of CAM development were not determined in our study, prior work reported that CAM completely encloses the egg at approximately 60-70% of the incubation (Webb et al., 1987; Stewart and Florian, 2000; Nechaeva et al., 2007). Nevertheless, CAM mass can continue to increase thereafter suggesting an expansion of the vascularization (Birchard and Reiber, 1993; Kam, 1993; Corona and Warburton, 2000; Blackburn et al., 2003). An increase in CAM vascularization late in incubation would then support the calculated increase hemoglobin saturation and allow greater surface area for oxygen loading which would also impact overall increase in egg VO_2 (Fig 1B). The relative cardiac output measurements showed that during the second half of incubation the fraction of CO directed to the yolk was very small further increasing the total amount flowing to embryonic tissues (Fig. 4). Over the final 30% of development the CAM vasculature received a considerable higher fraction (25-32%) of CO, when compared to 50% of incubation (Fig. 4). In comparison to other vertebrate groups this value was lower than that reported for late stage chicken embryos (44%; Mulder et al., 1997) and to the placenta fraction in near-term fetal sheep (41%; Jensen et al., 1991) however, this could be attributed to differences developmental temperature and overall metabolic demand. The increase in CO directed to the CAM from 50 to 70% incubation in snapping

turtles (Fig. 4A-B), may reflect a higher vascular density and an expanded surface for gas-exchange to occur. The majority of CO was directed to the embryo at all stages measured, although it was reduced at 70% in comparison to 50% and 90% incubation (Fig. 4). It is important to note that absolute values of blood flow to the organs were not determined due to limitations of the microsphere technique as reported by Mulder and colleagues (1997). The size of the snapping turtle embryo and their small blood volume restricted the collection of a reference blood sample simultaneously to the microspheres injection and absolute measures of blood flow proved unsuccessful.

Our estimates of CAM blood flow suggest an overall decrease at 90% incubation (Table 2). Also, the calculated relative cardiac output index indicated that mass specific cardiac output decreased throughout incubation, which was previously suggested to occur in developing turtles (Birchard and Reiber, 1996; Crossley and Burggren, 2009, Crossley et al., 2017a). This reduction could contribute to either a slowing, a plateau, or a decline in oxygen consumption previously reported for embryonic turtles (Ackerman, 1981; Booth and Astill, 2001; Reid et al., 2009; Thompson, 1993). In this study we found that the estimated CO decreased with the progressive increase in egg VO_2 , however embryonic mass-specific VO_2 decreased as well (Fig. 1C). Nevertheless, the increase in oxygen carrying capacity of the blood and the lower mass-specific VO_2 at late stages of development compensate for any CO decline in snapping turtles and therefore it would not compromise metabolic function.

In summary, our findings indicated snapping turtles embryos increase oxygen carrying capacity while COI and heart rate decrease late in development. While we lack sufficient data to definitively assign the change in mass-specific metabolic rate to changes in convective oxygen transport capacity our data do suggest that the two are correlated. If this pattern persisted into the final 10% of snapping turtle incubation it may contribute to the previously reported patterns of whole egg VO_2 during the final stages of embryonic development.

Acknowledgements

We thank Prof. Turk Rehn for aid with egg collection and Dr. Kevin Tate for help in egg and animal care.

Competing interests

The authors declare no competing or financial interests.

Author contributions

Conceptualization: D.A.C.; E.W.T.; Methodology and execution: M.R.S., Z.F.K., D.A.C.; Formal analysis: M.R.S.; Data curation: M.R.S., D.A.C.; E.W.T.; Supervision: D.A.C.; E.W.T.; A.S.A.; Funding acquisition: A.S.A.; D.A.C. All authors discussed the results and revised the manuscript.

Funding

This study was supported by the São Paulo Research Foundation (Fundação de Amparo a Pesquisa do Estado de São Paulo, FAPESP; no. 2013/05677-9 to A.S.A./M.R.S; no. 2012/06938-8 to A.S.A./E.W.T.) and the National Science Foundation, NSF IBN-IOS 0845741 to D.A.C. E.W.T. was a Visiting Researcher with the Science Without Borders Programme (CNPq 401061/2014-0 to F. T. Rantin/E.W.T.).

REFERENCE LIST

- Ackerman, R.A.** (1981). Oxygen consumption by sea turtle (*Chelonia*, *Caretta*) eggs during development. *Physiol. Zool.* **54** (3), 316-324.
- Alvine, T., Rhen, T. and Crossley II, D.A.** (2013). Temperature-dependent sex determination modulates cardiovascular maturation in embryonic snapping turtles *Chelydra serpentina*. *J. Exp. Biol.* **216**, 751–758.
- Aulie, A. and Kanui, T.I.** (1995). Oxygen consumption of eggs and hatchlings of the Nile crocodile (*Crocodylus niloticus*). *Comp. Bioch. Physiol.* **112A** (1), 99-102.
- Birchard, G.F.** (2000). An ontogenetic shift in the response of heart rates to temperature in the developing snapping turtle (*Chelydra serpentina*). *J. Therm. Biol.* **25**, 287–291.
- Birchard, G.F. and Reiber, C.L.** (1993). A comparison of avian and reptilian chorioallantoic vascular density. *J. Exp. Biol.* **178**, 245–249.
- Birchard, G.F. and Reiber, C.L.** (1995). Growth, metabolism, and chorioallantoic vascular density of developing snapping turtles (*Chelydra serpentina*): influence of temperature. *Physiol. Zool.*, **68** (5), 799-811.
- Birchard, G.F. and Reiber, C.L.** (1996). Heart rate during development in the turtle embryo: effect of temperature. *J. Comp. Physiol.* **166B**, 461–466.
- Blackburn, D.G., Johnson, A.R. and Petzold, J.L.** (2003). Histology of the extraembryonic membranes of an oviparous snake: towards a reconstruction of basal squamate patterns. *J. Exp. Zool.* **299A**, 48–58.
- Booth, D.T.** (1998a) Incubation of turtle eggs at different temperatures: do embryos compensate for temperature during development? *Physiol. Zool.* **71** (1), 23-26.
- Booth, D.T.** (1998b). Effects of incubation temperature on the energetics of embryonic development and hatchling morphology in the Brisbane river turtle *Emydura signata*. *J. Comp. Physiol.* **168B**, 399-404.
- Booth, D.T. and Astill, K.** (2001). Incubation temperature, energy expenditure and hatchling size in the green turtle (*Chelonia mydas*), a species with temperature-sensitive sex determination. *Aust. J. Zool.* **49** (4), 389 – 396.
- Booth, D.T. and Thompson, M.B.** (1991). A Comparison of reptilian eggs with those of megapode birds. In *Egg Incubation: Its Effects in Embryonic*

- Development in Birds and Reptiles* (ed. D.C. Deeming & M.W.J. Ferguson), p. 325-345, Cambridge: Cambridge Univ. Press.
- Booth, D.T., Thompson, M.B. and Herring, S.** (2000). How incubation temperature influences the physiology and growth of embryonic lizards. *J. Comp. Physiol.* **170B** (4), 269-276.
- Burggren, W., Farrell, A. and Lillywhite, H.** (2011) Vertebrate Cardiovascular Systems. In *Comprehensive Physiology* (ed. R. Terjung) doi: 10.1002/cphy.cp130104
- Corona, T.B. and Warburton, S.J.** (2000). Regional hypoxia elicits regional changes in chorioallantoic membrane vascular density in alligator but not chicken embryos. *Comp. Biochem. Physiol.* **125A** (1), 57–61.
- Crossley II, D.A.** (1999). Development of cardiovascular regulation in embryos of the domestic fowl (*Gallus gallus*), with partial comparison to embryos of the desert tortoise (*Gopherus agassizii*). PhD thesis, University of North Texas, Denton, TX.
- Crossley II, D.A. and Altimiras, J.** (2000). Ontogeny of autonomic control of cardiovascular function in the domestic chicken *Gallus gallus*. *Am. J. Physiol.* **279**, R1091-R1098.
- Crossley II, D.A. and Altimiras, J.** (2005). Cardiovascular development in embryos of the American alligator *Alligator mississippiensis*: effects of chronic and acute hypoxia. *J. Exp. Biol.* **208**, 31-39.
- Crossley II, D.A. and Burgreen, W.W.** (2009). Development of cardiac form and function in ectothermic Sauropsids. *J. Morphol.* **270**, 1400–1412.
- Crossley II, D.A., Smith, C., Harfush, M., Sánchez-Sánchez, H., Garduño-Paz, M.V. and Méndez-Sánchez, J.F.** (2017a). Developmental cardiovascular physiology of the olive ridley sea turtle (*Lepidochelys olivacea*) *Comp. Biochem. Physiol.* **211A**, 69–76.
- Crossley II, D.A., Ling, R., Nelson, D., Gillium, T., Conner, J., Hapgood, J., Elsey, R.M. and Eme, J.** (2017b). Metabolic responses to chronic hypoxic incubation in embryonic American alligators (*Alligator mississippiensis*). *Comp. Biochem. Physiol.* **203A**, 77-82. doi:10.1016/j.cbpa.2016.08.017
- Dmi'el, R.** (1970). Growth and metabolism in snake embryos, *J. Embryol. Exp. Morph.* **23** (3), 761-772.

- Du, W-G., Radder, R.S., Sun, B. and Shine, R.** (2009). Determinants of incubation period: do reptilian embryos hatch after a fixed total number of heart beats? *J. Exp. Biol.* **212**, 1302-1306.
- Eme, J., Altimiras, J., Hicks, J.W. and Crossley II, D.A.** (2011). Hypoxic alligator embryos: chronic hypoxia, catecholamine levels and autonomic responses of in ovo alligators. *Comp. Biochem. Physiol.* **160A**, 412–420.
- Eme J., Tate K.B., Kohl Z.F., Slay C.E., Hicks J.W., and Crossley II D.A.** (2012). Cardiovascular plasticity during hypoxic development in reptile embryos. *Integr. Comp. Biol.* **52**, E54-E54.
- Frair, W.** (1977). Turtle red blood cells packed volumes, sizes and numbers. *Herpetologica*. **33** (2), 167-190.
- Gettinger, R.D., Paukstis, G.L. and Gutzke, W.H.N.** (1984). Influence of hydric environment on oxygen consumption by embryonic turtles *Chelydra serpentina* and *Trionyx spiniferus*. *Physiol. Zool.* **57** (4), 468-473.
- Jensen, A., Roman, C., Rudolph, A.** (1991). Effects of reducing uterine blood flow on fetal blood flow distribution and oxygen delivery. *J. Dev. Physiol.* **15**, 309–323.
- Joyce, W., Elsey, R.M., Wang T., Crossley II, D.A.** (2018). Maximum heart rate does not limit cardiac output at rest or during exercise in the American alligator (*Alligator mississippiensis*). *Am. J. Physiol.* <https://doi.org/10.1152/ajpregu.00027.2018>
- Kam, Y.-C.** (1993). Physiological effects of hypoxia on metabolism and growth of turtle embryos. *Resp. Physiol.* **92**, 127–138.
- Lynn, W. G and Von Brand, T.** (1945). Studies on the oxygen consumption and water metabolism of turtle embryos. *Biol. Bull.* **88** (2), 112-125.
- McGlashan, J.K., Loudon, F.K., Thompson, M.B. and Spencer, R.J.** (2015). Hatching behavior of eastern long-necked turtles (*Chelodina longicollis*): the influence of asynchronous environments on embryonic heart rate and phenotype. *Comp. Biochem. Physiol.* **188A**, 58–64.
- Miller, K. and Packard, G.C.** (1992). The influence of substrate water potential during incubation on the metabolism of embryonic snapping turtles (*Chelydra serpentina*). *Physiol. Zool.* **65** (1), 172-187.

- Mulder, T.L.M., Golde, J.C., Prinzen, F.W. and Blanco, C.E.** (1997). Cardiac output distribution in the chick embryo from stage 36 to 45. *Cardiovasc. Res.* **34**, 525–528.
- Nechaeva, M.V., Vladimirova, I. G. and Alekseeva, T.A.** (2007). Oxygen consumption as related to the development of the extraembryonic membranes and cardiovascular system in the European pond turtle (*Emys orbicularis*) embryogenesis. *Comp. Biochem. Physiol.* **148A**, 599–610.
- Piiper, J., Tazawa, H., Ar, A. and Rahn, H.** (1980). Analysis of chorioallantoic gas exchange in the chick embryo. *Resp. Physiol.* **39**, 273-284.
- Reid, K.A., Margaritoulis, D. and Speakman, J.R.** (2009). Incubation temperature and energy expenditure during development in loggerhead sea turtle embryos. *J. Exp. Mar. Bio. Ecol.* **378**, 62-68.
- Sartori, M.R., Leite, C.A.C., Abe, A.S., Crossley, D.A. and Taylor, E.W.** (2015). The progressive onset of cholinergic and adrenergic control of heart rate during development in the green iguana, *Iguana iguana*. *Comp. Biochem. Physiol.* **188A**, 1–8.
- Sartori, M.R., Abe, A.S., Crossley, D.A. and Taylor, E.W.** (2017). Rates of oxygen uptake increase independently of changes in heart rate in late stages of development and at hatching in the green iguana, *Iguana iguana*. *Comp. Biochem. Physiol.* **205A**, 28-34.
- Spencer, R-J., Thompson, M.B. and Banks, P.B.** (2001). Hatch or wait? A dilemma in reptilian incubation. *Oikos*. **93**, 401–406.
- Stecyk, J.A.W., Overgaard, J., Farrell, A.P. and Wang, T.** (2004). α - Adrenergic regulation of systemic peripheral resistance and blood flow distribution in the turtle *Trachemys scripta* during anoxic submergence at 5°C and 21°C. *J. Exp. Biol.* **207**, 269-283.
- Stewart, J.R. and Florian, J.D.** (2000). Ontogeny of extraembryonic membranes of the oviparous lizard, *Eumeces fasciatus* (Squamata: Scincidae). *J. Morphol.* **244**, 81–107.
- Taylor, E.W., Leite, C.A.C., Sartori, M.R., Wang, T., Abe, A.S. and Crossley II, D.A.** (2014). The phylogeny and ontogeny of autonomic control of the heart and cardiorespiratory interactions in vertebrates. *J. Exp. Biol.* **217**, 690-703.

- Tazawa, H. and Mochizuki, M.** (1977). Oxygen analyses of chicken embryo blood. *Resp. Physiol.* **31**, 203-215.
- Thompson, M.B.** (1989). Patterns of metabolism in embryonic reptiles. *Resp. Physiol.* **76**, 243-256.
- Thompson, M.B.** (1993). Oxygen consumption and energetics of development in eggs of leatherback turtle, *Dermochelys coriacea*. *Comp. Bioch. Phys.* **104A**, 449-453.
- Thompson, M.B. and Russel, K.J.** (1998). Metabolic cost of development in one of the world's smallest lizard eggs: implications for physiological advantages of the amniote egg. *Copeia*. **1998**, 1016-1020.
- Thompson, M.B. and Russel, K.J.** (1999). Embryonic energetics in eggs of two species of australian skink, *Morethia boulengeri* and *Morethia adelaidensis*. *J. Herpet.* **33** (2), 291-297.
- Thompson, M.B. and Stewart, J.R.** (1997). Embryonic metabolism and growth in lizards of the genus Eumeces. *Comp. Biochem. Physiol.* **118A** (3), 647-654.
- Tucker, V.A.** (1967). Method for oxygen content and dissociation curves on microliter blood samples. *J. appl. Physiol.* **23** (3), 410-414.
- Vleck, C.M. and Hoyt, D.F.** (1991). Metabolism and energetics of reptilian and avian embryos. In *Egg Incubation: Its Effects in Embryonic Development in Birds and Reptiles* (ed. D.C. Deeming and M.W.J. Ferguson). Cambridge: Cambridge Univ. Press.
- Warburton, S.J., Hastings, D. and Wang, T.** (1995). Responses to chronic hypoxia in embryonic alligators. *J. Exp. Biol.* **273**, 44-50.
- Webb, G.J.W., Manolis, S.C., Whitehead, P.J. and Dempsey, K.** (1987). The possible relationship between embryo orientation opaque banding and the dehydration of albumen in crocodile eggs. *Copeia* **1987** (1), 252-257.
- Whitehead, P.J., Seymour R.S.** (1990). Patterns of metabolic rate in embryonic crocodilians *Crocodylus johnstoni* and *Crocodylus porosus*. *Physiol. Zool.* **63**, 334-352.
- Yntema, C.L.** (1968). A series of stages in the embryonic development of *Chelydra serpentina*. *J. Morphol.* **125**, 219-252.

Tables

Table 1. Changes in mass of snapping turtle embryos from 50%, 70% and 90% incubation.

Mass	50%	70%	90%
Egg (g)	12.4 ± 0.5 ^a	13.1 ± 0.4 ^a	13.4 ± 0.2 ^a
Yolk (g)	3.72 ± 0.15 ^a	2.71 ± 0.13 ^b	1.18 ± 0.07 ^c
Body (g)	1.62 ± 0.08 ^a	4.39 ± 0.13 ^b	7.16 ± 0.16 ^c
Heart (g)	0.007 ± 0.0002 ^a	0.017 ± 0.001 ^b	0.022 ± 0.001 ^c
Heart/Body (%)	0.46 ± 0.02 ^a	0.38 ± 0.01 ^b	0.31 ± 0.02 ^c
Liver (g)	0.047 ± 0.002 ^a	0.111 ± 0.006 ^b	0.213 ± 0.008 ^c
N	21	24	21

Data presented as means ± s.e.m. Different letters denote statistical difference among incubation periods.

Table 2. Blood oxygen carrying capacity properties and CAM cardiac output from snapping turtle embryos at 50%, 70% and 90% of incubation.

	50%	70%	90%	
Hct (%)	23.5 ± 1.4 (13) ^a	22.7 ± 1.5 (13) ^a	21.1 ± 0.9 (12) ^a	
[Hb] (mg/dl)	6.8 ± 0.2 (10) ^a	7.0 ± 0.4 (12) ^a	7.5 ± 0.4 (11) ^a	
PaO₂ (kPa)	-	3.0 ± 0.2 ^a	2.6 ± 0.3 ^a	
PaCO₂ (kPa)	-	3.2 ± 0.2 ^a	3.4 ± 0.3 ^a	
SaO₂ (%)	-	34% (5)	49% (5)	
Relative COI	0.28 ± 0.10 ^a	0.17 ± 0.04 ^b	0.14 ± 0.05 ^b	
%Q_{CAM}	9.2 ± 2.3 (5)	31.6 ± 3.7 (18)	25.3 ± 6.2 (15)	
Q_{CAM}(ml min⁻¹)	0.46	0.71	0.50	
Q_{CAM}(ml min⁻¹ g⁻¹)	0.33	0.17	0.07	
	50% - E (3)	50% - L (4)	70% (7)	90% (8)
Embryo mass (g)	1.8 ± 0.5 ^a	2.3 ± 0.5 ^a	4.4 ± 0.3 ^b	7.0 ± 0.1 ^c
P₅₀ 2% CO₂ (kPa)	6.72 ± 0.69 ^a	1.35 ± 0.11 ^b	1.25 ± 0.04 ^b	1.25 ± 0.05 ^b
P₅₀ 6% CO₂ (kPa)	6.25 ± 1.49 ^a	1.72 ± 0.15 ^b	1.67 ± 0.08 ^b	1.63 ± 0.05 ^b
Bohr shift	-0.19 ± 0.10 ^a	-0.47 ± 0.16 ^a	-0.46 ± 0.08 ^a	-0.49 ± 0.15 ^a
nH 2% CO₂	2.1 ± 0.1 ^a	2.1 ± 0.2 ^a	2.2 ± 0.1 ^a	2.4 ± 0.1 ^a
nH 6% CO₂	1.8 ± 0.3 ^a	2.0 ± 0.5 ^a	2.1 ± 0.1 ^a	2.4 ± 0.1 ^a

Hematocrit (Hct%); hemoglobin concentration [Hb]; cardiac output index calculated based on cardiac mass (relative COI); proportion of cardiac output directed to the CAM calculated by the microspheres distribution (%Q_{CAM}); cardiac output calculated with the Fick Equation (Q_{CAM}), partial pressure of oxygen at 50% hemoglobin saturation (P₅₀); Hill coefficient (nH). Data derived from the oxygen dissociation curves at 50% incubation (P₅₀, Bohr shift and nH) were divided in two subgroups, early (50% - E) and late (50% - L). All data presented as means ± s.e.m. Different letters denotes statistical significance among incubation periods; sample size is given in parenthesis.

Figures

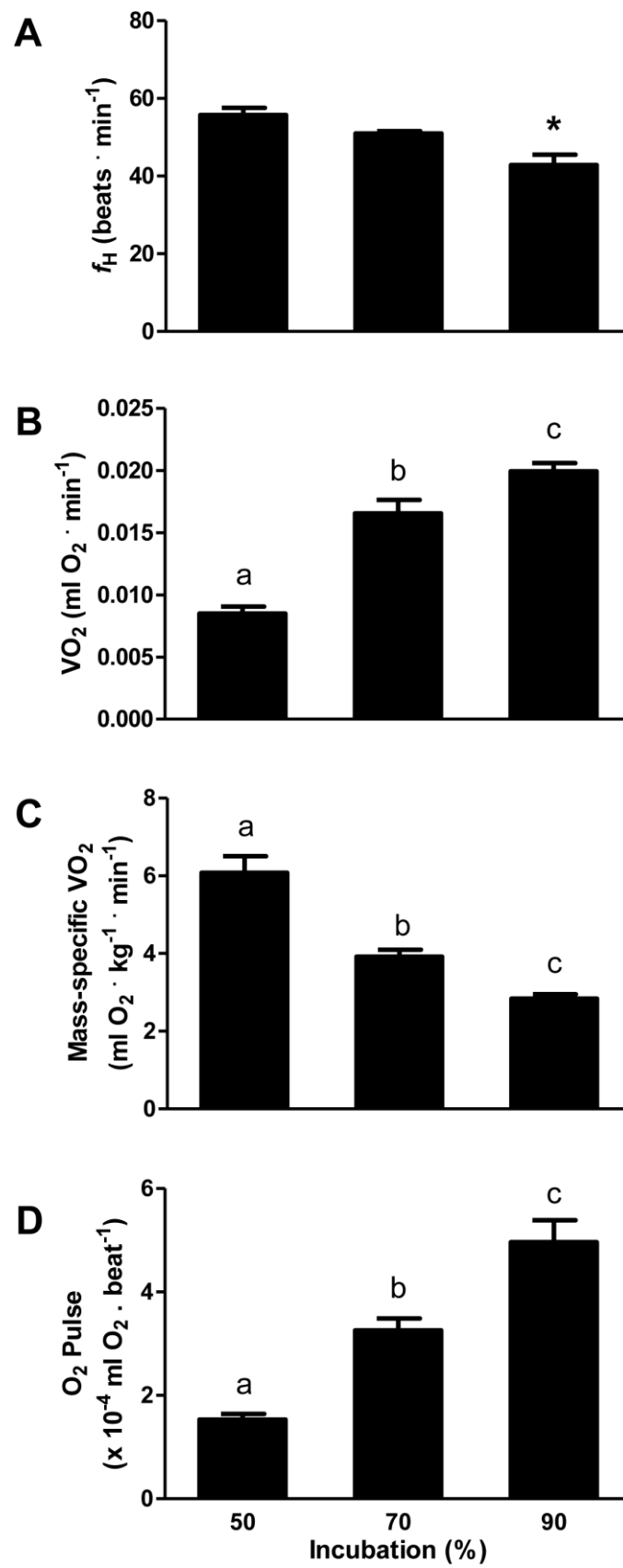


Fig. 1 f_H , VO_2 , mass-specific VO_2 and mass-specific O_2 pulse from snapping turtles at 50, 70 and 90% incubation. **A)** Mean heart rates (beats min^{-1}) and s.e.m. bars of embryonic turtles at different times of incubation period. At 90% the rate is lower than at 50% and 70% ($P < 0.001$). **B)** Total oxygen consumption ($\text{ml } O_2 \cdot \text{min}^{-1}$) of *C. serpentina* eggs at 50%, 70% and 90% of the incubation period. The volume of oxygen consumed increased progressively throughout incubation period ($P < 0.001$); **C)** Embryonic mass-specific VO_2 ($\text{ml } O_2 \cdot \text{kg}^{-1} \cdot \text{min}^{-1}$). The rate of oxygen consumption per gram of embryo decreased progressively with the increase in embryonic mass ($P < 0.001$); **D)** Mass-specific oxygen pulse ($\text{ml } O_2 \cdot \text{beat}^{-1} \cdot \text{kg}^{-1}$) calculated from mass-specific VO_2 and f_H data. Mass-specific oxygen pulse decreased at 90% of development ($P < 0.001$).

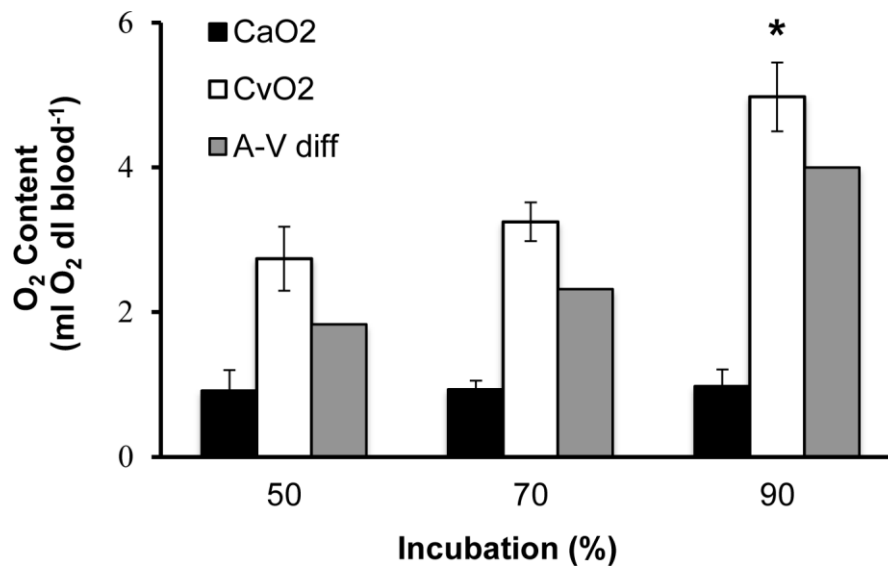


Fig 2 Blood oxygen content of embryonic snapping turtles at 50, 70 and 90% incubation. Mean blood oxygen content in arteries (CaO₂, black bars) and veins (CvO₂, white bars) of the choriollantoic membrane of snapping turtle embryos, and the resulting A-V diff (grey bars). Arterial mixed blood oxygen content did not vary through development ($P=0.824$), but venous blood oxygen content increased at 90% of development ($P<0.05$). Arterial mixed oxygen content was higher than venous content at every incubation period tested (t-test; $P<0.02$).

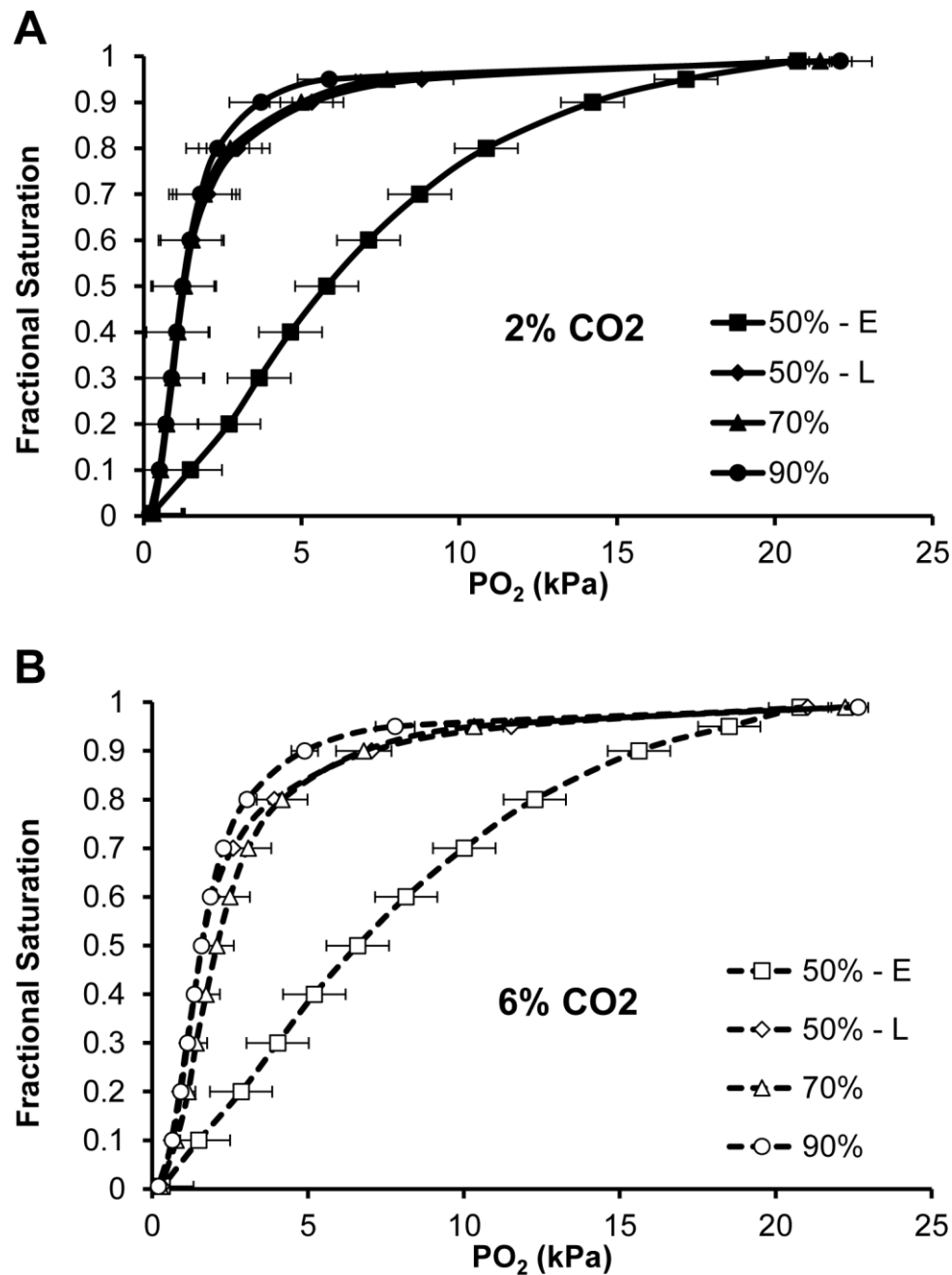


Fig. 3 Oxygen equilibrium curves from snapping turtles at 50, 70 and 90% incubation at different CO₂ conditions. A) Samples were deoxygenated with N₂ mixed with 2% CO₂ (similar to oxygenated blood; closed markers) or B) 6% CO₂ (similar to deoxygenated blood; open markers) and the saturation calculated from the fraction of deoxyhemoglobin. Early 50% (50% - E; squares), late 50% (50% - L; diamonds), 70% (triangles) and 90% (circles).

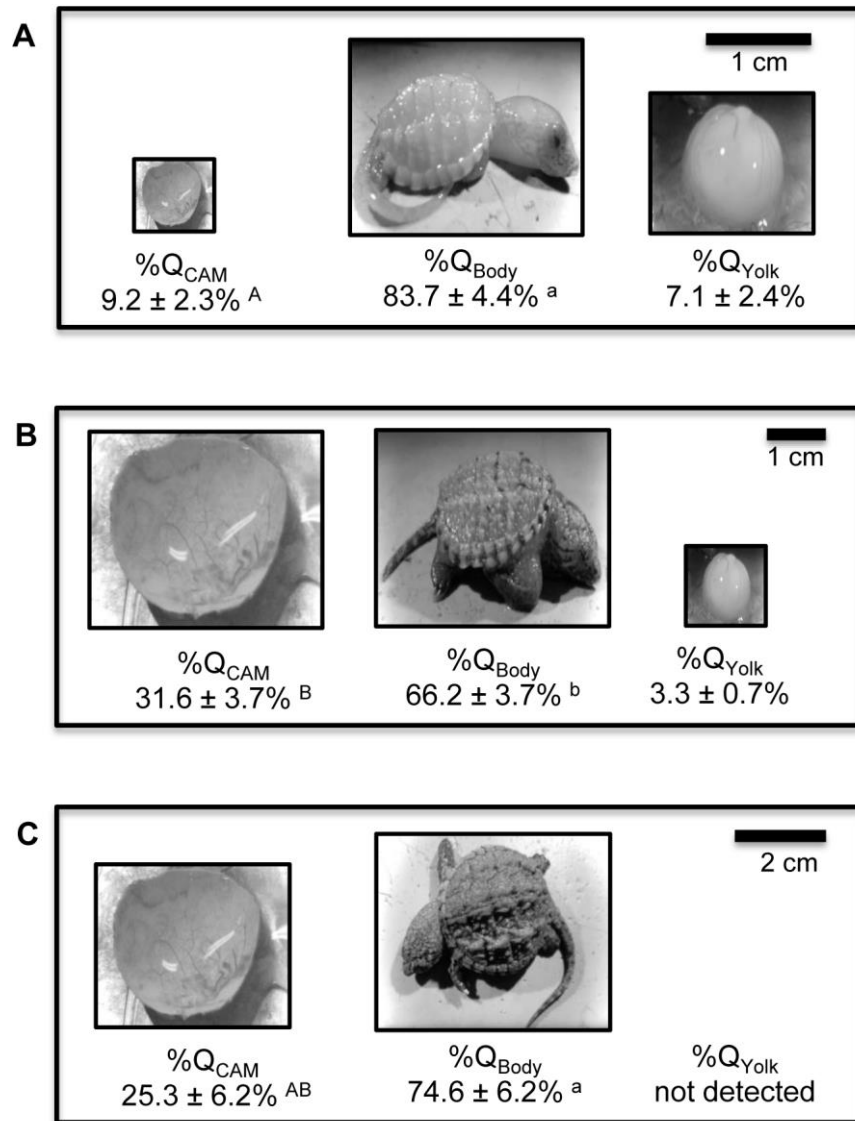


Fig. 4 Relative cardiac output distribution in embryonic snapping turtles at 50, 70 and 90% incubation. Percentages of relative blood flow or systemic cardiac output (%Q_{sys}): embryonic tissues (%Q_{BODY}); chorioallantoic membrane (%Q_{CAM}); and yolk sac (%Q_{YOLK}) during routine normoxia at 30°C. **A**) 50% incubation (N=5), **B**) 70% incubation (N=18 for %Q_{CAM} and %Q_{BODY} and N=11 for %Q_{YOLK}) and **C**) 90% incubation (N=15). Values of systemic cardiac output (%Q) were obtained with the microspheres study. The different sizes of the of yolk and CAM images are to illustrate the different fractions of %Q_{sys}. Scale bars are depicted in each figure.